Internal Reference Electrode in Dye Sensitized Solar Cells for Three-Electrode Electrochemical Characterizations

A. Zaban,*,† J. Zhang,† Y. Diamant,† O. Melemed,† and J. Bisquert*,‡

Department of Chemistry, Bar-Ilan University, Ramat-Gan 52900, Israel, and Departament de Ciències Experimentals, Universitat Jaume I, 12080 Castelló, Spain

Received: March 4, 2003; In Final Form: May 13, 2003

A new design of dye-sensitized solar cells that contains an internal reference electrode enables detailed electrochemical characterization of the cells at the practical operating configuration. A thin insulating gap splits the nanoporous TiO_2 electrode in twin halves, one serving as the active electrode in the solar cell and the other one as a photoreference that maintains the open circuit potential. This configuration allows separation of the two components of the cell potential, that of the photoactive electrode and that in the counter electrode, while maintaining the practical sandwich configuration. Analysis of efficient solar cells shows that the contributions of the counter electrode to the energy losses are larger than expected. By intentionally decreasing the counter electrode quality, we observed a modification of the photocurrent at the same effective electrode potential. This result is explained in terms of the coupling between the hole collection efficiency at the counter electrode and the recombination currents at the active electrode.

Introduction

A dye sensitized solar cell (DSSC) is a photoelectrochemical system. Its operation is based on the photoinjection of electrons from dye molecules into an inorganic semiconductor and hole transfer to a redox mediator.[1−3] The low light absorption by a dye monolayer and the low injection efficiency of dye multilayers necessitate the use of a high surface area, nanoporous semiconductor electrode.[4] The photoinjected electrons reach the external circuit via the nanoporous semiconductor network, whereas the holes in the form of oxidized ions transit through the electrode pores toward the counter electrode.

Most DSSCs are constructed in the sandwich configuration.[1−3] That is, the nanoporous dye sensitized electrode is pressed against the counter electrode while the electrolyte fills the pores by capillary forces. In this configuration, the distance between the two electrodes is less than 20 μm and the electrolyte layer beyond the porous semiconductor is even thinner. Consequently, the vast majority of DSSC research is done in a 2-electrode configuration where the electrochemical potential is determined with respect to the counter electrode.[1−3,5,6]

In the absence of a reference electrode, any electrochemical characterization of the solar cell represents the whole system without the ability to differentiate the specific contribution of each electrode. The interpretation of electrochemical measurements is further complicated by the fact that the potential of the counter electrode (which is also the reference) is determined by the electrolyte composition.[7] In the common DSSC, the counter electrode is made of materials that catalyze the redox reaction thus maintaining the electrolyte potential.[1,8−11] However, the electrode potential may shift depending on the operating conditions of the cell. For example, the electrolyte composition changes between open circuit conditions and short circuit operation, which in turn alters the counter/reference electrode potential.

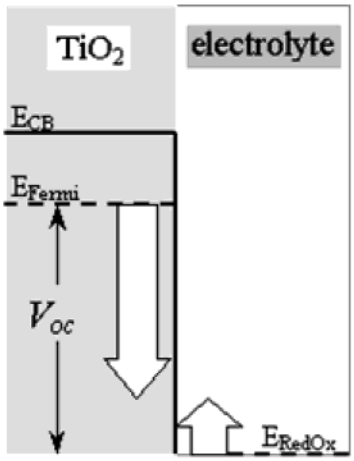

Figure 1. Energy diagram of a DSSC during a scan from open circuit potential to the short circuit conditions, illustrating the possible shift of the electrolyte/counter electrode potential.

To illustrate the importance of a 3-electrode configuration, we examine the most basic characterization method of a solar cell: the photocurrent−voltage dependence (the iV curve). Figure 1 presents an energy diagram of a DSSC during a scan from open circuit potential (V_{oc}) to the short circuit (J_{sc}) conditions. As mentioned above, in a standard 2-electrode DSSC, the cell voltage is referred to the counter electrode potential, which except for dark open circuit conditions is not defined. Compared with dark conditions, only a small change of the electrolyte composition is expected at open circuit under illumination. The exact change depends on the number of electrons present in the nanoporous semiconductor and the initial ratio between the redox components. However, as the voltage is scanned toward short circuit, the photocurrent density increases and ion concentration gradients are built in the cell. Depending on the photocurrent density and counter electrode

* To whom correspondence should be addressed. E-mail: zabana@mail.biu.ac.il (A.Z.); bisquert@exp.uji.es (J.B.).
† Bar-Ilan University.
‡ Universitat Jaume I.

10.1021/jp034554a CCC: $25.00
Published on Web 05/30/2003

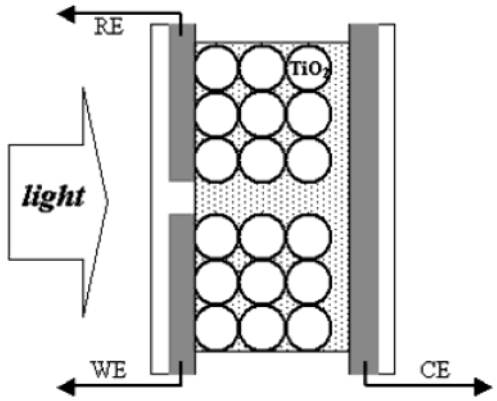

Figure 2. Schematic presentation of the 3-electrode DSSC. The standard 2-electrode measurement is performed using the working (sensitized) and counter electrodes. For a 3-electrode measurement of the same cell, the reference electrode maintaining Voc is added.

quality, a shift of the electrolyte potential near the counter electrode that also serves as a reference is likely to happen.

The standard way to incorporate a reference electrode in DSSCs necessitates a separation of the sensitized electrode from the counter thus increasing the cell volume by a large factor.[12−15] However, the volume increase alters the cell operation significantly as the total amount of ions, concentration gradients, and transit distances in the cell change. Consequently, the standard 3-electrode setup of DSSCs exhibits a poor simulation of an operating cell.

We report here on the fabrication of DSSCs that contain an internal reference electrode thus enabling a 3-electrode measurement under operating conditions. The 3-electrode cell is a standard DSSC except that the sensitized electrode (including the transparent conducting layer) is split by a narrow nonconducting gap. The cell design, presented in Figure 2, enables one to perform two kinds of measurements of the DSSC performance. First, using one-half of the sensitized electrode and the counter electrode, we determine the electrochemical properties of the whole cell, i.e., a 2-electrode measurement that includes the counter electrode contribution. Second, using the same configuration, we employ the second half of the sensitized electrode as a reference that maintains open circuit potential. Using a potentiostat, we ensure that no current flows through the reference electrode during the measurement. Thus, the potential of the photoreference electrode is maintained constant and the electrochemical properties of this 3-electrode DSSC are measured versus defined potentials.

Experimental Section

The DSSCs measured in this study had the standard sandwich-type configuration in which a dyed nanoporous TiO_2 electrode is facing a Pt counter electrode. However, in contrast to the standard cells, the nanoporous TiO_2 electrode was split in half by a narrow nonconducting gap resulting in two parts that are electrically disconnected.

The synthesis and characterization of the TiO_2 colloidal paste (20 nm diameter crystals) is reported elsewhere.[16] The conductive glass substrates (Libby Owens Ford, 15 ohm/square F-doped SnO_2) were cleaned with soap, rinsed with deionized water, and dried in a nitrogen stream. The TiO_2 colloid paste was spread over the substrate with a glass rod using adhesive tape as spacers. The films were fired at 450 °C for 30 min in air resulting in 4 μm thick film. After the firing, a narrow nonconducting gap was made across the electrode using a fine ceramic glass scraper. The gap resistance was higher than 100 MΩ. To ensure that no TiO_2 is left in the gap a control experiment was done using conductive substrates that were disconnected electrically prior to the TiO_2 deposition by laser etching. In this case, adhesive tape was placed on the gap before the TiO_2 deposition and the separation was ca. 1 mm.

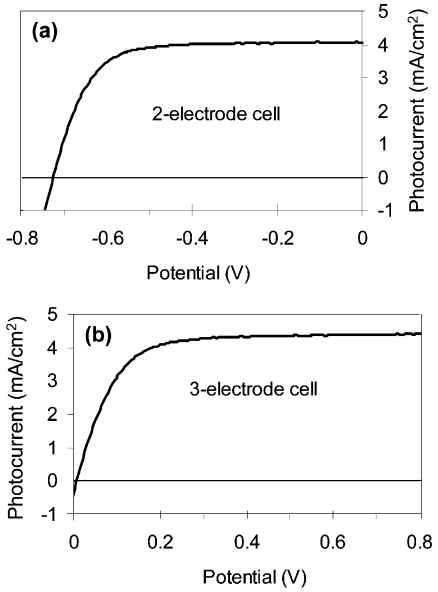

Figure 3. iV curves of (a) the 2-electrode and (b) the 3-electrode DSSC. The potentials are measured versus the counter electrode potential in the 2-electrode configuration, and versus the open circuit potential (V_{oc}) in the 3-electrode setup. Note that the potential scales are shifted by the V_{oc} value.

The dye (*cis*-di(isothiocyanato)-*N*-bis(4,4′-dicarboxy-2,2′-bipyridine) ruthenium(II)) was adsorbed by immersing the TiO_2 electrodes overnight in a 0.5 mM ethanol solution of the dye. As a counter electrode, we used a Pt coated F-doped SnO_2 film. 0.5 M LiI/ 0.05M I_2 in 1:1 acetonitrile: NMO (3-methyl-2-oxazolidinone) was used as an electrolyte.

Illumination of the cell was done using a calibrated Xe lamp. An Eco Chemie potentiostat was used to measure the photocurrent−voltage correlation. The film thickness was measured with a profilometer (Mitutoyo, Surftest SV 500).

Results and Discussion

Figure 3a presents the iV curve of the DSSC presented in Figure 2, measured in the standard 2-electrode configuration. The cell voltage is measured versus the counter electrode. The cell performance is characterized by $V_{oc} = 725$ mV, $J_{sc} = 4.07$ mA/cm^2, and a fill factor (FF) = 71%. Figure 3b presents the iV curve of the same cell in a 3-electrode configuration. Here the potential is measured versus the photoreference electrode that maintains the open circuit potential (V_{oc}). The potential scales of Figure 3, parts a and b, are shifted by the V_{oc} value.

Figure 4 presents the two iV curves of Figure 3 on a common potential scale. For convenience, we use the standard 2-electrode presentation in terms of voltage. In practice, the 3-electrode curve was shifted negatively by the V_{oc} value ensuring that the zero current points match. The 3-electrode curve resembles a cell having J_{sc} that is higher by 8% compared with the 2-electrode measurement. When normalized to similar J_{sc}, the iV curves differ mainly at voltages negative than −0.5 V.

In a standard electrochemical system, the data presented in Figure 4 could be described as the practical iV curve and the pure sensitized electrode contribution to this curve, both under operating conditions. This description relates the difference

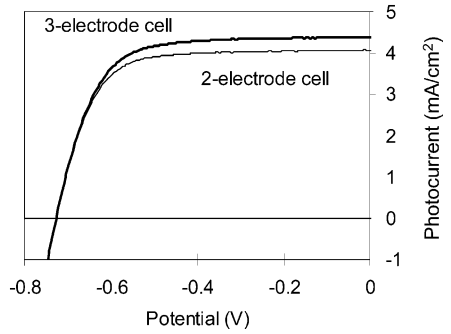

Figure 4. iV curves of the 2 and 3-electrode measurements of the DSSC presented in Figure 3. The potential of the 3-electrode cell was shifted to the standard (2-electrode) presentation.

between the iV curves to a potential drop at the counter electrode. That is, the lower photocurrent obtained at the 2-electrode cell throughout the voltage scan results from a negative shift of the counter electrode with respect to the open circuit conditions. Depending on the catalytic quality of the counter electrode and the current density in the cell, the potential of the counter electrode, which serves also as a reference, shifts negatively thus altering the *effective* potential at the sensitized electrode. The gradual shift of the effective potential affects the shape of the iV curve and the observed fill factor. According to this approach, one could measure the potential drop at the counter electrode by standard electrochemical methods thus estimating the role of the counter electrode in the cell operation.[7,9] Consequently, one may assume that the iV curves measured in 2-electrode cells could be corrected for the counter electrode shifts.

In practice, it is often assumed that an efficient counter electrode does not affect the cell performance. However, as shown in Figure 4, this is hardly the case even for a system that generates relatively low photocurrents. The reason for that is probably related to the thin layer configuration. The electrochemical measurements done in a bulky setup cannot resemble the DSSC conditions that more likely obey thin layer electrochemistry.[17]

In the simplest approach, the iV curve of DSSCs can be modeled by a diode equation.[18] That is, the iV curve under illumination is the sum of a constant photocurrent and a recombination current that is independent of illumination and equals the dark current. However, this simple model is known to fail for real DSSCs. At a given potential, the dark current is much smaller than the recombination current under illumination (obtained by subtracting the short-circuit current from the measured current).[19] Furthermore, it was noted that the increase of the current toward more positive potential is slower than exponential.[20] These characteristics cannot be simulated by fitting with reasonable series resistance. The diode equation has to be modified by an effective barrier height that depends on the current.[20,21]

In the remainder of the paper, we show that the new 3-electrode measurement reveals a more complicated situation. In addition to the potential drops, which affect the iV characteristics of the 2-electrode cell, the counter electrode influences the overall cell performance via the recombination mechanism of the solar cell. This recombination contribution is often more significant than the potential drops. As in the case of the potential drops, the role of the counter electrode in the recombination processes depends on the quality of the counter electrode and it cannot be calculated from independent electrochemical measurement of the counter electrode.

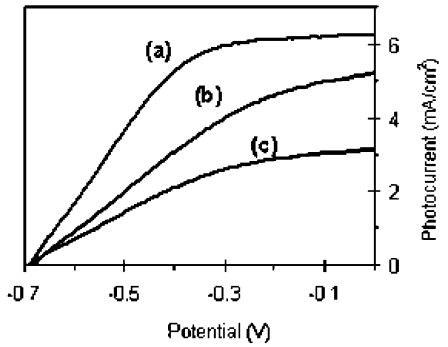

Figure 5. Three iV curves measured in a 3-electrode configuration using the same sensitized electrode and different counters. The different photocurrents obtained at similar applied voltages are attributed to recombination processes resulting from the counter electrode quality.

Figure 5 shows three iV curves measured in a 3-electrode configuration using the same sensitized electrode but different counter electrodes that differ by their catalytic quality. In practice, the Pt coating of the counter electrode was damaged by gradual polishing going from curve 5a to 5c. The decrease of the counter electrode quality resulted in the following observations: First, the difference between the iV curves measured in the 3-electrode configuration and those measured by the 2-electrode setup increased with respect to several factors: the short circuit currents, the curves' shapes and the fill factors (not shown). The second observation seems surprising at first. Despite the 3-electrode setup, the measured photocurrents decreased as the counter electrode was made less catalytic. In other words, at the same *effective* potential of the working (sensitized) electrode, the photocurrent was affected by the counter quality.

Unlike the first observation, the second one cannot be explained by the potential drops ideas discussed with respect to Figure 4. Thus, the lower photocurrents associated with the less catalytic counters are attributed to the low regeneration (reduction) efficiency of the electrolyte which increases the recombination rate in the solar cell. The recombination rate depends on the electron concentration/potential at the sensitized electrode and on the concentration of oxidized ions in the electrolyte. The potentials of the sensitized electrode in all three cells are similar when the 3-electrode configuration is used. However, the electrolyte composition can vary. In other words, the results presented in Figure 5 resemble a direct measurement of the recombination process. A simple illustration of this concept relates to the short circuit photocurrents of the cells presented in Figure 5. Moving from cell 5a to 5c, the short circuit photocurrent decreases to about half of its original value although the potential of the sensitized electrode is not changed. This significant decrease can be explained only by the higher recombination currents induced by the slower holes collection (redox regeneration) at the counter electrode. Consequently, one can study the recombination process by a direct measurement of the recombination current as a function of the sensitized electrode potential.

Summary

The internal photoreference electrode presented in this work is a simple but powerful tool for the study of DSSCs. A correlation between 2-electrode and 3-electrode measurements provides information regarding the quality of the counter electrode and possible potential drops in the system. The analysis of iV curves of DSSCs should be simplified significantly by the 3-electrode measurement. Furthermore, other electrochemical

and photoelectrochemical measurements of the cell like impedance spectroscopy or intensity modulated photovoltage/current spectroscopies should benefit from the possibility to define the potential of the sensitized electrode.

We showed that a comparison between different cells measured in the 3-electrode setup provides direct information on the recombination processes that are associated with the electrolyte composition. The development of a model that enables full analysis of the iV characteristics in this case is currently under progress.

Acknowledgment. We acknowledge the support of this work by the Israeli Ministry of Science and the Fundació Caixa Castelló (project P11B2002-39).

References and Notes

(1) Gratzel, M. *Prog. Photovoltaics* **2000**, *8*, 171.

(2) Cahen, D.; Hodes, G.; Gratzel, M.; Guillemoles, J. F.; Riess, I. *J. Phys. Chem. B* **2000**, *104*, 2053.

(3) Ellingson, R. J.; Asbury, J. B.; Ferrere, S.; Ghosh, H. N.; Sprague, J. R.; Lian, T. Q.; Nozik, A. J. *J. Phys. Chem. B* **1998**, *102*, 6455.

(4) Gerfin, T.; Gratzel, M.; Walder, L. Molecular and Supermolecular Surface Modification of Nanocrystalline TiO2 Films: Charge Separating and Charge Injecting Devices. In *Molecular Level Artificial Photosynthetic Materials*; Karlin, K. D., Ed.; John Wiley & Sons: New York, 1997; Vol. 44; pp 345−393.

(5) de Jongh, P. E.; Meulenkamp, E. A.; Vanmaekelbergh, D.; Kelly, J. J. *J. Phys. Chem. B* **2000**, *104*, 7686.

(6) Ferrere, S.; Gregg, B. A. *J. Phys. Chem. B* **2001**, *105*, 7602.

(7) Oskam, G.; Bergeron, B. V.; Meyer, G. J.; Searson, P. C. *J. Phys. Chem. B* **2001**, *105*, 6867.

(8) Hagfeldt, A.; Gratzel, M. *Acc. Chem. Res.* **2000**, *33*, 269.

(9) Papageorgiou, N.; Maier, W. F.; Gratzel, M. *J. Electrochem. Soc.* **1997**, *144*, 876.

(10) Hauch, A.; Georg, A. *Electrochim. Acta* **2001**, *46*, 3457−3466.

(11) Peter, L. M.; Duffy, N. W.; Wang, R. L.; Wijayantha, K. G. U. *J. Electroanal. Chem.* **2002**, *524*−*525*, 127−136.

(12) Yan, S. G.; Hupp, J. T. *J. Phys. Chem. B* **1997**, *101*, 1493.

(13) Kamat, P. V.; Bedja, I.; Hotchandani, S.; Patterson, L. K. *J. Phys. Chem.* **1996**, *100*, 4900−4908.

(14) Cao, F.; Oskam, G.; Searson, P. C.; Stipkala, J. M.; Heimer, T. A.; Farzad, F.; Meyer, G. J. *J. Phys. Chem.* **1995**, *99*, 11974.

(15) Kuciauskas, D.; Freund, M. S.; Gray, H. B.; Winkler, J. R.; Lewis, N. S. *J. Phys. Chem. B* **2001**, *105*, 392.

(16) Zaban, A.; Aruna, S. T.; Tirosh, S.; Gregg, B. A.; Mastai, Y. *J. Phys. Chem. B* **2000**, *104*, 4130.

(17) Bard, A. J.; Faulkner, L. R. *Electrochemical Methods Fundamental and Applications*; John Wiley & Sons: New York, 1980.

(18) Sodergren, S.; Hagfeldt, A.; Olsson, J.; Lindquist, S. E. *J. Phys. Chem.* **1994**, *98*, 5552−5556.

(19) Huang, S. Y.; Schilchthörl, G.; Nozik, A. J.; Grätzel, M.; Frank, A. J. *J. Phys. Chem B* **1997**, *101*, 2576−2582.

(20) Dittrich, T. *Phys. Status Solidi (a)* **2000**, *182*, 447−455.

(21) Dittrich, T.; Beer, P.; Koch, F.; Weidmann, J.; Lauermann, I. *Appl. Phys. Lett.* **1998**, *73*, 1901−1903.